RESEARCH

Analysis of monthly average precipitation of Wadi Ouahrane basin in Algeria by using the ITRA, ITPAM, and TPS methods

**Mohammed Achite · Gokmen Ceribasi · Andrzej Wałęga ·
Ahmet Iyad Ceyhunlu · Nehal Elshaboury · Nir Krakauer · Tarek Hartani ·
Tommaso Caloiero · Sajid Gul**

Abstract Precipitation is one of the most significant components for the basin's hydrological cycle. Numerous features of a basin's water circulation may be affected by the chronological, geographical, and seasonal fluctuation of precipitation. It could be an important factor that influences hydrometeorological phenomena including floods and droughts. In this research, the innovative trend risk analysis (ITRA), innovative trend pivot analysis (ITPAM), and trend polygon star (TPS) methodologies of visualizing precipitation data are used to detect precipitation changes at six stations in Algeria's Wadi Ouahrane basin from 1972 to 2018. ITRA graphs show the direction of the precipitation trend (increasing–decreasing) and the trend risk class. Disparities in the polygons generated by the arithmetic mean and standard deviation ITPAM graphs demonstrate variations in precipitation seasonally and in the seasonal precipitation trends (increasing or decreasing) between sites. The TPS maps depict monthly variations in precipitation and highlight the autumn and spring transitions between the dry and wet seasons.

M. Achite
Laboratory of Water & Environment, Faculty of Nature and Life Sciences, University Hassiba Benbouali of Chlef, Ouled Fares, 02180 Chlef, P.B 78C, Algeria

M. Achite · T. Hartani
National Higher School of Agronomy, ENSA, 16200 Algiers, Algeria

G. Ceribasi · A. I. Ceyhunlu
Faculty of Technology, Department of Civil Engineering, Sakarya University of Applied Sciences, Sakarya 54187, Turkey

A. Wałęga
Department of Sanitary Engineering and Water Management, University of Agriculture in Krakow, Mickiewicza 24/28 Street, 30-059 Krakow, Poland

N. Elshaboury
Construction and Project Management Research Institute, Housing and Building National Research Centre, Giza 12311, Egypt

N. Krakauer
Department of Civil Engineering, the City College of New York, New York 10031, USA

T. Hartani
Morsli Abdellah Tipaza University Center, Oued Merzoug, 42000 Tipaza, Algeria

T. Caloiero
Institute for Agriculture and Forest Systems in the Mediterranean (CNR-ISAFOM), National Research Council of Italy, Via Cavour 4/6, 87036 Rende, CS, Italy

S. Gul (✉)
School of Mathematics and Statistics, Zhengzhou University, Zhengzhou 450001, China
e-mail: sgqaustat@gmail.com

Springer

Introduction

Precipitation is the basic input parameter to the water balance of a hydrologic basin. The temporal and spatial variability as well as the seasonality of precipitation can affect water circulation over the basin and, in consequence, be a significant factor that determines hydrometeorological phenomena like drought and floods. Thus, precipitation has a strong impact on humans, society, infrastructure, and the ecosystem (Collins et al., 2013). Climate change projections also showed that precipitation variability can increase and can lead to the more frequent occurrence of drought and water scarcity, mainly in the region where the agriculture sector plays an important role in water demand. Research has indicated that excessive rainfall has indeed intensified due to human-caused warming in the twentieth century (Zhang et al., 2013) and a further increase is visible and projected throughout the twenty-first century (Toreti et al., 2013; Pendergrass & Hartmann, 2014; Asadieh & Krakaur, 2015). The variability of precipitation can be determined by atmospheric circulation (Młyński et al., 2018) on the relevant scale such as monsoons, the jet stream, or tropical and extratropical cyclone tracks, and orographic barriers (Nishant & Sherwood, 2021). In the case of the Mediterranean region, North Atlantic Oscillation (NAO) teleconnection patterns (Kingston et al., 2015; Littmann, 2000) and sea surface temperature (SST) anomalies (Hu & Wang, 2021; Zhang & Wu, 2021) can influence strong variability of precipitation.

In this paper, we focused on analyzing changes in precipitation on the Wadi Ouahrane basin in Algeria. In this region, knowledge about trends and variability of precipitations is very important because of the intensity of agriculture and restricted supply of water. Door (2011) claimed that Algeria's renewable fresh water reserves are quite limited and therefore can be projected at 19 billion m^3 per year. The water resources are equivalent to 450 m^3 per capita per year that's somewhat less than the 500 m^3 per capita per year specified as the scarcity threshold signaling an impending water shortage (Achite et al.,

2021a). Within this context, several works analyzed the variability of precipitation and its link with the atmospheric circulation in Algeria. An analysis of rainfall and hydrometric regimes was performed on the Cheliff (west Algeria) and Medjerda (east Algeria) basins over the period 1968–2013 evidencing a strong correlation between the NAO and the precipitation (Khedimallah et al., 2020). As regards Northern Algeria, Taibi et al. (2017) linked the changes in annual precipitation, identified since the 1970s, with the El Niño Southern Oscillation (ENSO) which, as pointed out by Zeroual et al. (2017), resulted positively correlated with rainfall in this area. At the same time, in western Algeria, the temporal variability of the annual precipitation has been identified as influenced by the ENSO (Meddi et al., 2010) and the NAO (Tramblay et al., 2013). Moreover, the NAO and the ENSO have been identified as responsible for the significant changes of rainfall variability detected in the Northeastern Algeria (Turki et al., 2016) and northern central Algeria (Zerouali et al., 2018).

One of the essential topics in the analyses of hydrometeorological phenomena is detecting direction changes. Such changes can be examined to show the role of natural and anthropogenic factors. The detected trend of precipitation has a huge role in water availability in the basin and can help examine drought on a temporal and spatial scale. Several parametric and non-parametric methods have been proposed and described in literature for trend analysis (Praveen et al., 2020), and new methodologies such as continuous wavelet method have been proposed in order to identify the interannual modes controlling the rainfall variability (Turki et al., 2016). Anyway, in general, trend analysis relies on non-parametric tests, including the Mann–Kendall or Sen's slope assessments, which are more acceptable than parametric ones for non-normally distributed data (Ali & Abubaker, 2019; Croitoru & Toma, 2010; Onyutha, 2016; Zhao et al., 2019). These tests have some limitations, linked with the null hypothesis (H_0) (Blain, 2013), which assumes no serial correlation of data (Wang et al., 2020; Yue & Wang, 2004). According to Serinaldi et al. (2018), even while empirical trend estimation using basic statistical tests is always numerically possible, it has inadequate non-stationary information sources without requiring a priori further knowledge about the underlying stochastic process. Qualitative methods have been developed to visualize changes that may not

be seen using standard statistics, which can then be quantified and studied further. These methods include innovative test analysis (ITA) (Şen, 2012), innovative polygon trend analysis (IPTA), and innovative triangular trend analysis (ITTA) (Almazroui & Şen, 2020; Ceribasi & Ceyhunlu, 2021; Ceribasi et al., 2021a).

Achite et al. (2021b) investigated IPTA technique to identify precipitation patterns at seven locations in the Wadi Sly basin, Algeria, during a fifty-year period (1968–2018). The inquiry found that the IPTA method, the Mann–Kendall test, and Sen's estimator yielded results that were in satisfactory correlation. Moreover, the IPTA is easy to perform and has a low computational cost in comparison to other methods. The innovative trend pivot analysis method (ITPAM) is a new variation on this concept, where it is possible to visualize not only seasonally specific trend direction but also the strength of trend expressed as a risk degree (Ceribasi et al., 2021a, b). Finally, the trend polygon star (TPS) method can show seasonal transitions of analyzed hydrometeorological phenomena during the study period, unlike classical non-parametric and parametric tests. One of the main limitations of classical trend analysis is the lack of information about the transition of hydroclimatic variables between months, and thus, using tests does not detect these phenomena (Harka et al., 2021; Kisi & Ay, 2014). The new approaches can address this gap and may be useful in preliminary studies, supporting results from and motivating classical statistical tests. Therefore, this research study aims to apply ITRA, ITPAM, and TPS to detect trends and transitions of mean monthly precipitation on the Wadi Ouahrane basin of northern Algeria. The novelty of this study is using ITRA, ITPAM, and TPS to capture seasonally specific temporal behavior of precipitation in this region of semiarid northwest Africa, where so far, the analysis has not been performed.

Materials and methods

Study area

The studied region is the Wadi Ouahrane basin in northern Algeria, which lies between 36°00′N and 36°24′N and between 01°00′E and 01°3′E. The 270 km² region is a portion of the Wadi Cheliff basin (see Fig. 1). The map of the research area is derived from a digital elevation model with a horizontal resolution of 12.5 ms. The map depicts a maximum altitude of 991 m and a minimum altitude of 165 m. Wadi Ouahrane is a minor tributary of the Wadi Cheliff. This basin is managed by six precipitation-measuring stations. The Wadi Ouahrane basin is bounded by the Wadi Fodda basin to the east, the Wadi Ras basin to the west, the Wadi Allala basin to the north, and the Wadi Sly basin to the south. It has a Mediterranean climate with an average interannual precipitation of 333 mm from 1972 to 2018. The mean yearly temperature is 18 °C. The precipitation series database utilized in this study contains monthly information obtained at six sites between 1972 and 2018 (Fig. 1 and Table 1). These precipitation data were taken from the Algerian National Water Resources Agency (NWRA) and the National Meteorological Organization (NMO).

Data collection and statistical analysis

Table 2 displays monthly and annual precipitation statistics for the Wadi Ouahrane basin. According to these statistics, winter is the wettest season for all stations, with over 50% of the yearly precipitation falling during this season.

Innovative trend risk analysis method

The ITA method was first introduced by Şen (2012). This method presented by Sen has become one of the most common methods used in the analysis of hydrometeorological data in recent years. The trend between the values of the data is determined by this method. In addition, the distinguishing feature of the innovative trend method from other trend tests is that it can analyze data sets that are short (Şen, 2012, 2013). In this study, a different approach is presented by adding risk classes to the ITA method for the first time. With this approach, ITRA divides the data into two equal series. The divided series are ordered from smallest to largest, and the data are arranged on the Cartesian system as in Fig. 2. In addition, the ITRA graph is divided into 5 equal parts, and the risk class of the data is determined.

When the ITRA graph given in Fig. 2 is examined, it is seen that there is a decreasing trend at the 5th, 4th, 3rd, and 2nd risk levels, respectively, in the 0–30, 30–60, 60–90, and 90–120 mm precipitation
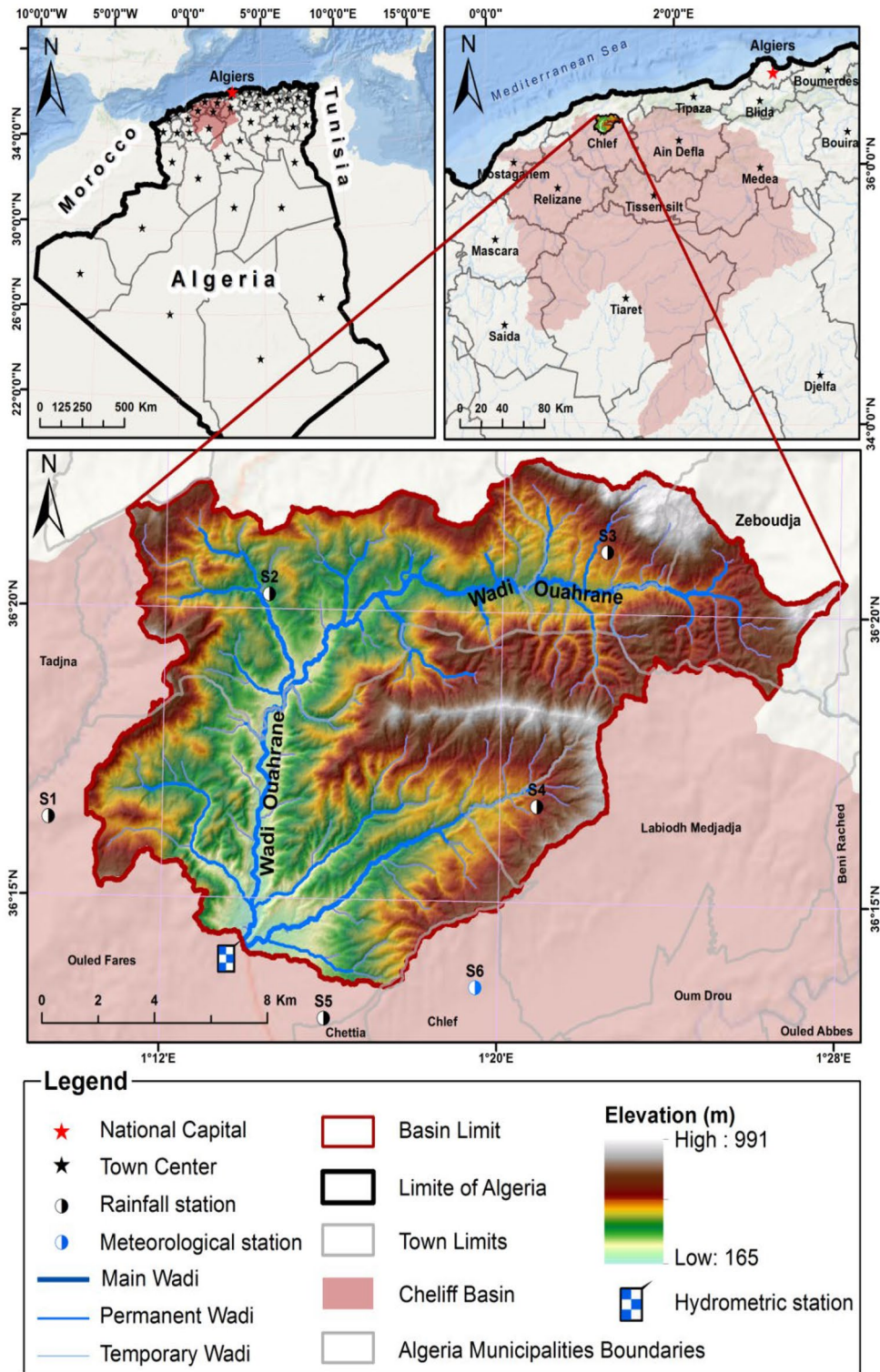
Fig. 1 Location, topographic characteristics, and pluviometric and hydrometric network of the study area

Stations	ID	Name	Geographical coordinates		Elevation
			Longitude	Latitude	
			(° ′ ″)	(° ′ ″)	(m)
S1	012,201	Larbat Ouled Fares	01°09′18″	36°16′20″	116
S2	012,224	Bouzghaia	01°14′27″	36°20′15″	217
S3	012,205	Benairia	01°22′28″	36°21′04″	320
S4	012,221	Medjaja	01°20′53″	36°16′39″	487
S5	012,209	Chettia	01°15′53″	36°12′56″	108
S6	NMO	Airport, Chlef	01°19′28″	36°13′31″	158

Table 1 Characteristics of the meteorological rainfall stations

range. On the other hand, it is concluded that there is an increasing trend at the 1st risk level in the precipitation range of 120–150 mm.

Innovative trend pivot analysis method

ITPAM is a trend visualization method based on the earlier IPTA method. The analysis of any data set is evaluated based on two different graphics generated by this method that show mean seasonal behavior across two halves of a data set. Examples of these two graphs for hypothetical monthly data are shown in Fig. 3 (Ceribasi et al., 2021a).

The graph on the left side of Fig. 3 shows the analysis result of a monthly data set by "risk ranges." As can be seen in Fig. 3, the range of the data values (and thus the *x*- and *y*-axes of the ITPAM graph) is divided into five equal parts. Risk ranges are formed with this division and range from 1st degree to 5th degree. The risk range of any month can be seen with this graph for the first and second half of the time series, and the magnitude of the change between the two halves can be readily discerned. The graph on the right side of Fig. 3 is recolored to distinguish ascending from descending trends for each month of the year. Moreover, this increasing or decreasing trend information is displayed in five different regions, designated as "high degree (HD)," "low degree (LD)," "very high degree (VHD)," "medium degree (MD)," and "very low degree (VLD)." If any data point lies on the 1:1 (45°) line, it is evaluated as "no trend (NT)." Alternative partitioning is also possible to classify trend regions in more detail.

Trend polygon star concept method

This is a trend analysis method developed by Sen (2021). This method analyzes the distance in the space of the hydrological variable, such as precipitation amount, between any 2 consecutive months of the year. The coordinate axis is divided into four regions, where the distance between any 2 months is within these four regions, and evaluation is made on these regions. The analysis result produced for a hypothetical monthly data set by this method is given in Fig. 4.

As seen in Fig. 4, the coordinate axis is divided into four regions. Arrows formed in these four regions are drawn from the origin point. For monthly studies, the transition between any two months is reflected in the length of this arrow line. The longer the size of the arrow line, the greater the transition between any 2 months is. The values on the vertical and horizontal axes of arrows, showing the transition between any 2 months, show a change in the first half of the data set compared to the second half (Ceribasi et al., 2021b). When the hypothetical analysis result shown in Fig. 4 is examined, arrows showing the transition between months J-J, A-S, S–O, and O-N are in region I. Therefore, both data halves show an increasing trend between these respective months. Arrows showing the transition between M-A and M-J months are in region II. Therefore, the first dataset shows a decreasing trend, while the second dataset shows an increasing trend. Arrows showing the transition between J-F and D-J months are in region III. Therefore, both data sets of these months show a decreasing trend. Arrows showing the transition between A-M, J-A, and N-D months are in region IV. Therefore, the first dataset shows an increasing trend, while the second dataset

Table 2 Descriptive statistics of monthly and annual precipitation in the Wadi Ouahrane basin (1972–2018)

Stations	Measures	S	O	N	D	J	F	M	A	M	J	J	A	An
S1	Min (mm)	0.00	0.30	0.00	0.00	0.00	0.00	0.00	0.00	0.00	0.00	0.00	0.00	207.50
	Max (mm)	85.20	120.60	134.40	167.60	143.90	164.50	116.40	135.80	111.50	65.00	8.70	11.60	628.00
	Mean (mm)	17.64	33.43	48.62	49.84	48.55	50.51	40.35	38.35	25.69	7.56	1.36	1.60	363.51
	SD (mm)	18.70	27.83	30.01	36.57	30.83	37.80	30.53	33.84	24.83	12.03	2.45	2.73	95.36
	CV	106.01	83.24	61.73	73.36	63.50	74.83	75.68	88.23	96.66	159.20	179.45	170.48	26.23
	C (%)	4.85	9.20	**13.37**	**13.71**	**13.36**	**13.90**	11.10	10.55	7.07	2.08	0.38	0.44	100.00
S2	Min (mm)	0.00	0.00	0.00	0.00	0.00	0.00	0.00	0.00	0.00	0.00	0.00	0.00	234.40
	Max (mm)	93.00	153.30	336.40	252.80	213.67	224.40	200.80	165.60	157.40	26.10	8.60	37.90	749.46
	Mean (mm)	20.95	37.47	73.78	73.73	67.84	67.96	57.61	47.41	31.97	4.68	0.73	2.71	486.83
	SD (mm)	22.07	35.15	61.81	58.52	44.41	53.73	47.67	40.51	38.02	5.85	2.05	6.35	129.83
	CV	105.35	93.79	83.77	79.37	65.47	79.06	82.75	85.46	118.92	125.03	282.42	234.13	26.67
	C (%)	4.30	7.70	**15.15**	**15.14**	**13.94**	**13.96**	11.83	9.74	6.57	0.96	0.15	0.56	100.00
S3	Min (mm)	0.00	0.50	0.00	1.50	0.00	0.04	0.12	0.00	0.00	0.00	0.00	0.00	163.20
	Max (mm)	77.27	105.30	156.30	118.30	140.00	143.30	105.10	137.27	132.30	63.00	12.78	30.30	588.20
	Mean (mm)	15.07	28.96	45.19	41.88	41.98	50.20	35.90	37.16	26.17	6.10	1.33	3.78	333.72
	SD (mm)	17.98	27.28	31.28	25.65	30.69	38.12	25.01	35.12	27.65	11.36	2.70	7.67	98.29
	CV	119.30	94.20	69.23	61.24	73.10	75.94	69.67	94.49	105.64	186.13	203.56	202.92	29.45
	C (%)	4.52	8.68	**13.54**	**12.55**	**12.58**	**15.04**	10.76	11.14	7.84	1.83	0.40	1.13	100.00
S4	Min (mm)	0.00	0.00	0.00	0.00	6.20	0.00	0.00	0.00	0.00	0.00	0.00	0.00	207.20
	Max (mm)	51.10	146.26	140.50	161.51	175.05	147.46	111.30	137.33	99.40	33.74	10.70	41.30	590.30
	Mean (mm)	16.75	34.44	56.75	53.35	51.78	57.92	42.73	38.81	25.97	6.67	1.41	3.16	389.73
	SD (mm)	12.31	29.18	34.18	36.93	33.09	43.46	28.25	32.42	27.81	7.98	2.72	7.20	90.43
	CV	73.53	84.74	60.23	69.22	63.90	75.04	66.11	83.53	107.09	119.60	193.30	228.00	23.20
	C (%)	4.30	8.84	**14.56**	**13.69**	**13.29**	**14.86**	10.96	9.96	6.66	1.71	0.36	0.81	100.00
S5	Min (mm)	0.00	0.00	1.20	0.00	10.00	0.00	0.00	0.00	0.00	0.00	0.00	0.00	238.64
	Max (mm)	61.40	182.15	265.10	182.64	124.03	177.48	114.49	196.15	100.48	47.50	18.84	51.00	624.92
	Mean (mm)	15.89	41.14	67.48	59.15	50.59	59.18	46.08	47.02	25.44	5.91	2.05	5.30	425.24
	SD (mm)	10.93	37.42	41.75	45.08	24.91	47.90	28.18	45.71	25.63	9.26	4.49	9.63	99.21
	CV	68.80	90.96	61.87	76.20	49.24	80.94	61.16	97.21	100.75	156.56	219.04	181.64	23.33
	C (%)	3.74	9.68	**15.87**	**13.91**	**11.90**	**13.92**	10.84	11.06	5.98	1.39	0.48	1.25	100.00

Table 2 (continued)

Stations	Measures	S	O	N	D	J	F	M	A	M	J	J	A	An
S6	Min (mm)	0.00	0.50	0.00	0.10	0.00	0.00	0.40	0.10	0.00	0.00	0.00	0.00	222.60
	Max (mm)	74.30	132.00	172.30	152.40	106.00	146.10	131.00	158.20	97.80	65.00	14.00	40.70	620.60
	Mean (mm)	18.91	38.55	54.99	50.85	46.44	60.65	46.61	44.22	30.57	9.43	1.98	4.34	407.53
	SD (mm)	18.51	33.08	35.25	36.26	25.08	44.35	30.09	38.30	27.53	13.29	3.39	8.71	102.39
	CV	97.91	85.82	64.09	71.31	54.01	73.12	64.55	86.62	90.08	140.88	171.58	200.78	25.12
	C (%)	4.64	9.46	**13.49**	**12.48**	**11.40**	**14.88**	11.44	10.85	7.50	2.31	0.48	1.06	100.00

Bold entries show the maximum value of C

SD standard deviation, C (%), monthly contribution, in percentage, to the total annual precipitation

shows a decreasing trend. These latter regions, II and IV, highlight possible changes in the seasonal cycle over the time spanned by the plotted data.

Results

Monthly average precipitation data of six stations (Larbat Ouled Fares, Bouzghaia, Benairia, Medjaja, Chettia, and Airport, Chlef) of Wadi Ouahrane basin are analyzed by three methods (i.e., ITRA, ITPAM, and TPS). The monthly average precipitation data analyzed by the ITRA method is given in Fig. 5.

When the ITRA graphs given in Fig. 5 are examined, there is no trend in the 0–30 mm precipitation range at Larbat Ouled Fares station; there is an increasing trend at the 4th risk level in the 30–70 mm precipitation range; it is concluded that there is a decreasing trend at the 3rd, 2nd, and 1st risk levels, respectively, in the precipitation range of 70–100 mm, 100–145 mm, and 145–180 mm. At Bouzghia station, there is a decreasing trend at the 5th risk level in the 0–45 mm precipitation range; it was concluded that there is an increasing trend at the 4th, 3rd, 2nd, and 1st risk levels, respectively, in the precipitation range of 45–105 mm, 105–170 mm, 170–225 mm, and 225–270 mm. At Benairia station, there is an increasing trend at the 5th and 4th risk levels in the 0–70 mm and 70–150 mm precipitation range and a decreasing trend at the 3rd and 2nd risk levels in the 150–200 mm and 200–225 mm precipitation range; it is concluded that there is an increasing trend at the 2nd and 1st risk levels, respectively, in the precipitation range of 225–300 mm and 300–350 mm. At Medjaja station, there is no trend in the 0–40 mm precipitation range, an increasing trend in the 4th risk level in the 40–75 mm precipitation range, and an increasing trend in the 3rd risk level in the 75–105 mm precipitation range; it was concluded that there is a decreasing trend at 3rd and 2nd risk levels, respectively, in the precipitation range of 105–125 mm and 125–170 mm and an increasing trend at the 1st risk level in the precipitation range of 170–200 mm. At Chettia station, there is no trend in the 0–30 mm precipitation range; there is an increasing trend at the 4th and 3rd risk levels, respectively, in the 30–75 mm and 75–105 mm precipitation range; it is concluded that there is a decreasing trend at the 3rd risk level in the 100–125 mm precipitation range and
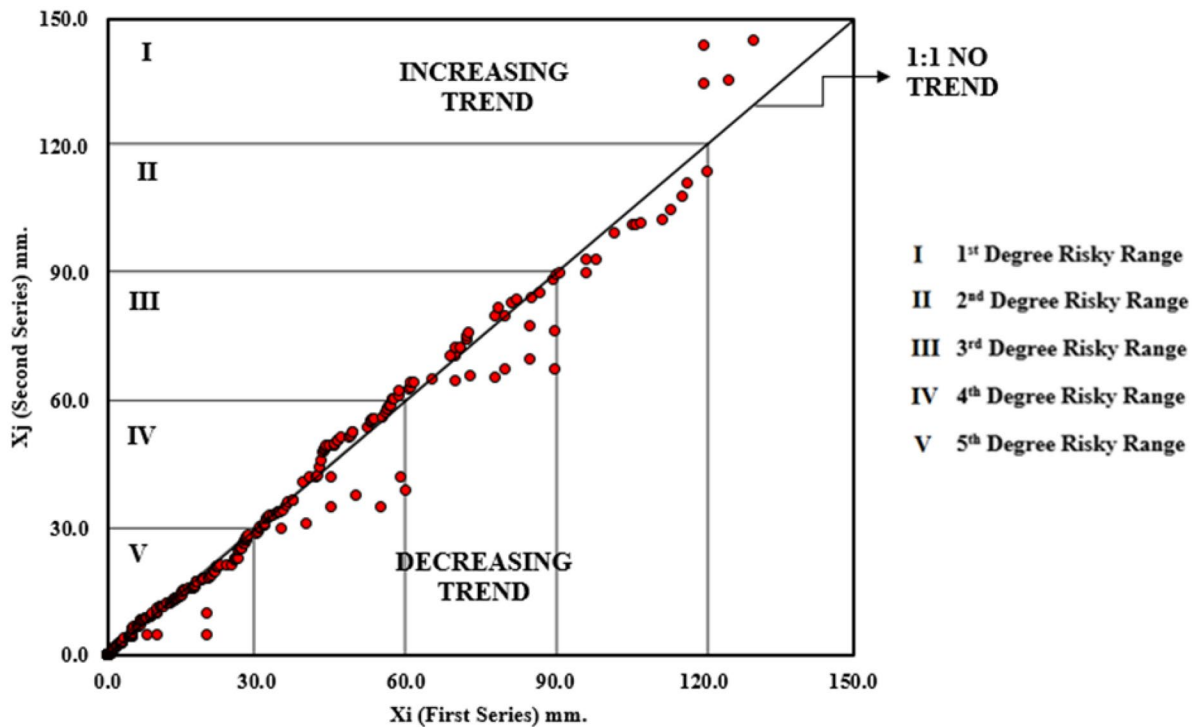
Fig. 2 Hypothetical ITRA for monthly data

an increasing trend at the 2nd and 1st risk levels in the 125–175 mm precipitation range. At Airport Chlef station, there is no trend in the 0–30 mm precipitation range; there is an increasing trend in the 4th, 3rd, 2nd, and 1st risk levels, respectively, in the 30–75 mm, 75–105 mm, 105–145 mm, and 145–160 mm precipitation range; it is concluded that there is a decreasing trend at the 1st risk level in the 160–175 mm precipitation range.

The analysis procedure performed for monthly average precipitation data is selected and applied to both the arithmetic mean and interannual standard deviation of monthly precipitation. Figure 6 displays the findings of ITPAM's arithmetic mean analysis. The analytical results for each site presented in Fig. 6 are assessed individually, and a summary assessment for each station is provided in Table 3.

Examining the arithmetic mean findings of ITPAM for each station listed in Table 3 produces the following conclusions. Differences in the precipitation seasonal cycle and its trend between stations are evident as different polygon shapes. Increasing or decreasing trends are seen as the deviation from the

1:1 (45°) line for most months and stations. While October is a medium-degree decreasing trend region, April is in a medium-degree increasing trend region. Meanwhile, November is in a high-degree increasing trend region, and no trend is seen in July. For all stations, June, July, and August are in the 5th risk range because precipitation is low. In contrast, November is in the 1st risk range for all stations because precipitation is relatively high and increasing between the two halves of the time series. For Larbat Ouled Fares station, while April is in a medium-degree increasing trend region, the risk range is 2nd degree. In particular, January, February, November, and December fall within the 1st degree of risk. February at Bouzghaia station is in a decreasing trend region of medium degree, although the risk range is 2nd degree. Meanwhile, November falls inside the first degree of risk. While March is in a somewhat dropping trend region for the Benairia station, the threat level is 2nd degree. In addition, November falls inside the 1st degree of risk. For the stations of Medjaja and Chettia, since March is in a region with a medium-degree declining trend, the risk range is 2nd degree. Moreover,
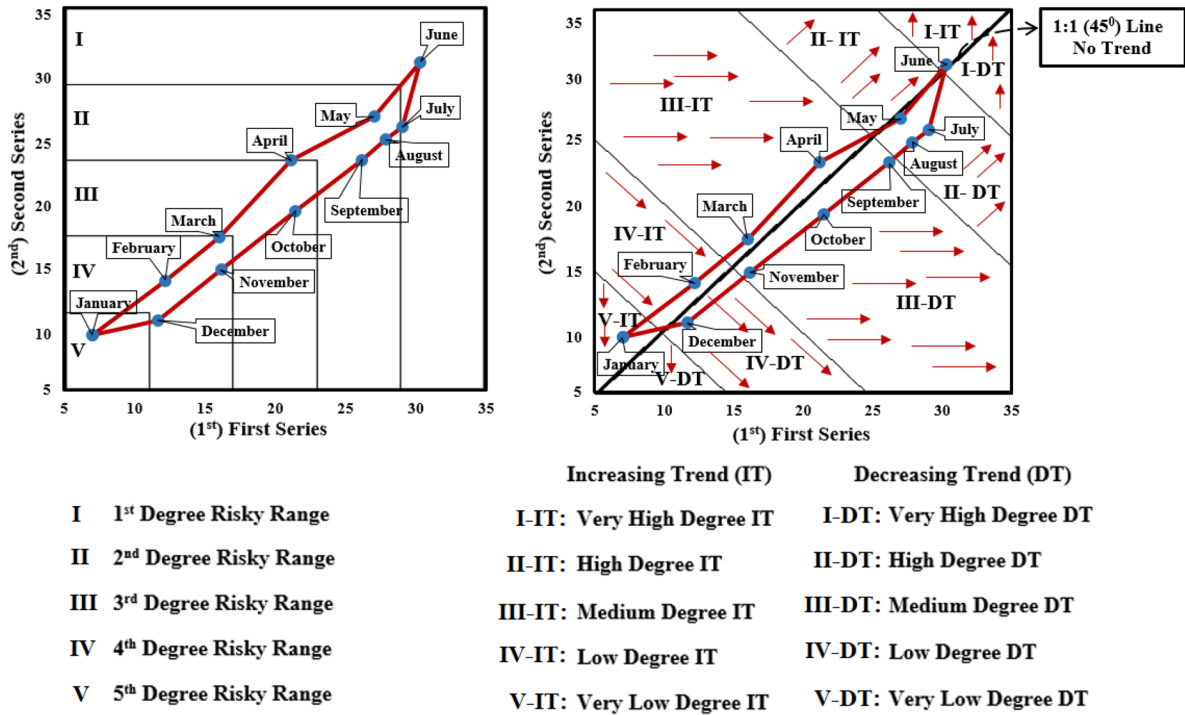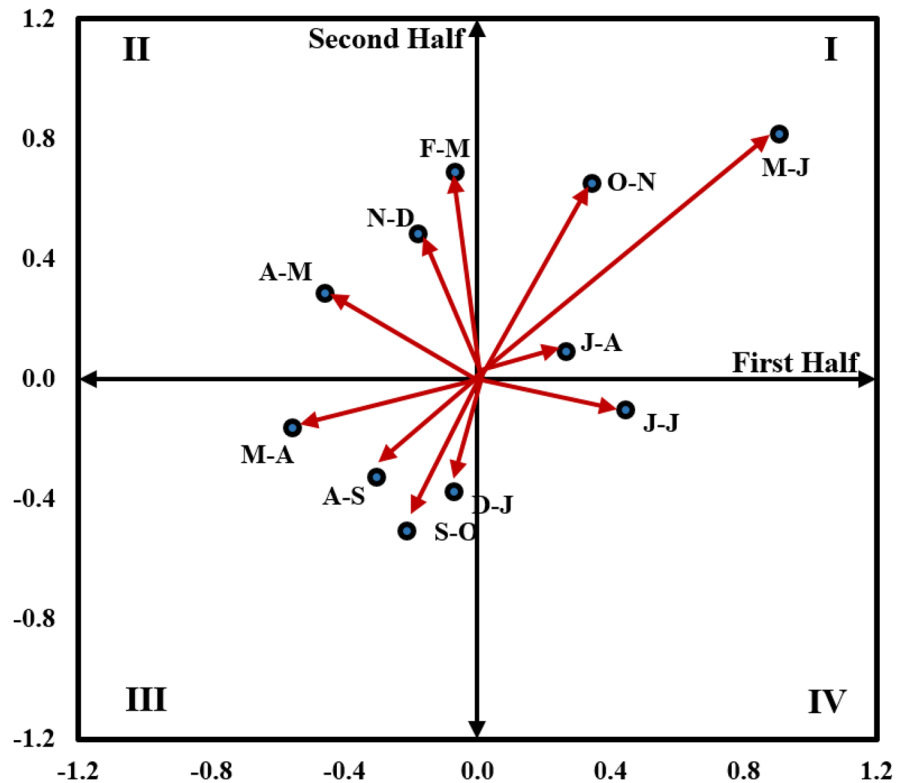
Fig. 3 Hypothetical ITPAM for monthly data

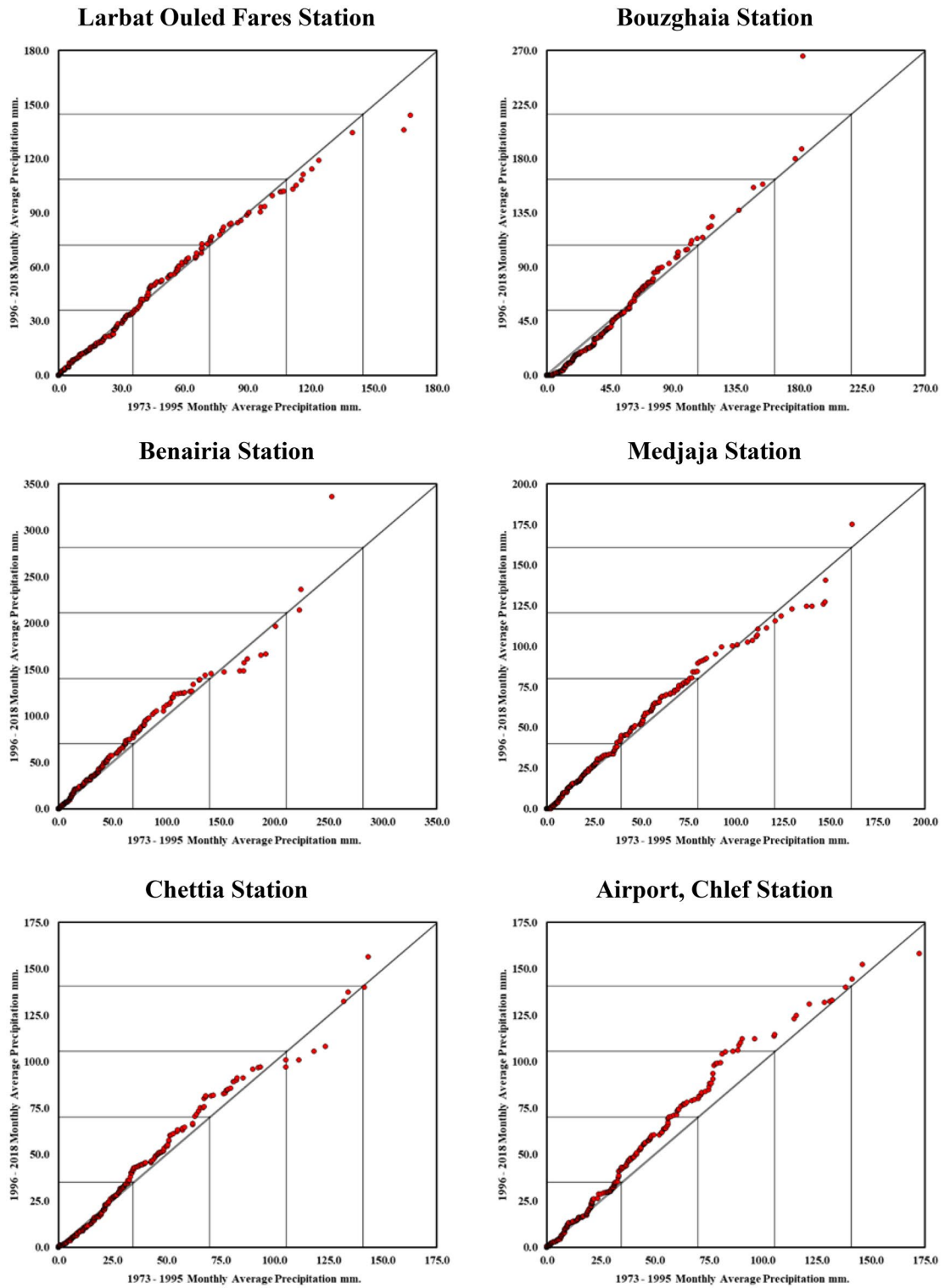**Fig. 4** Hypothetical trend polygon star concept method for monthly data

Larbat Ouled Fares Station

Bouzghaia Station

Benairia Station

Medjaja Station

Chettia Station
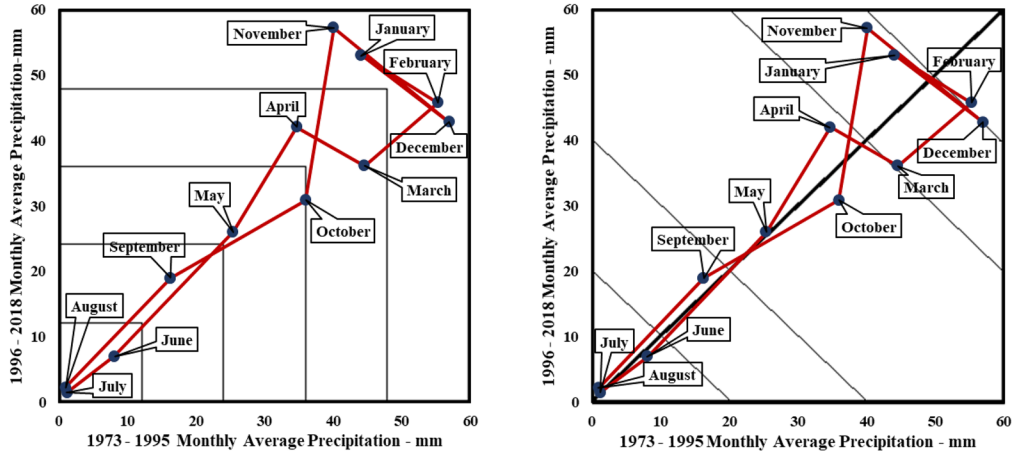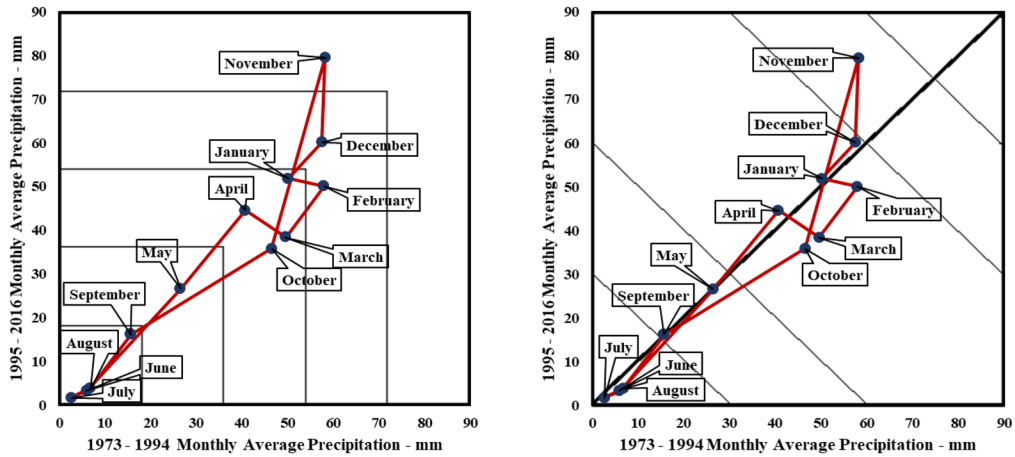
Airport, Chlef Station

Fig. 5 Arithmetic mean analysis results of ITRA for each station

Larbat Ouled Fares Station
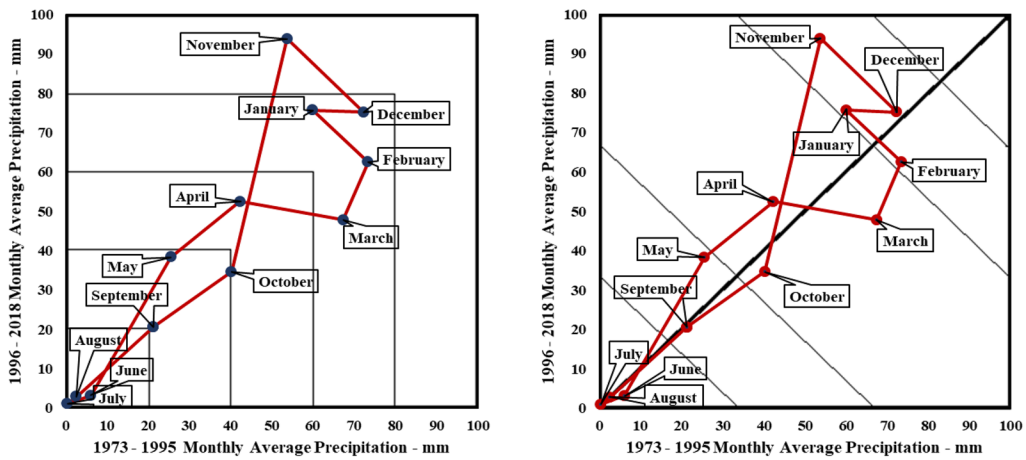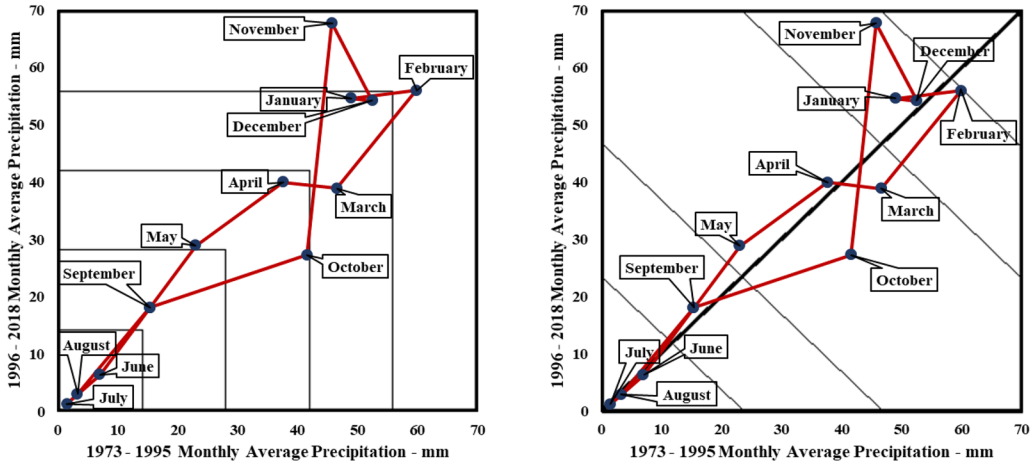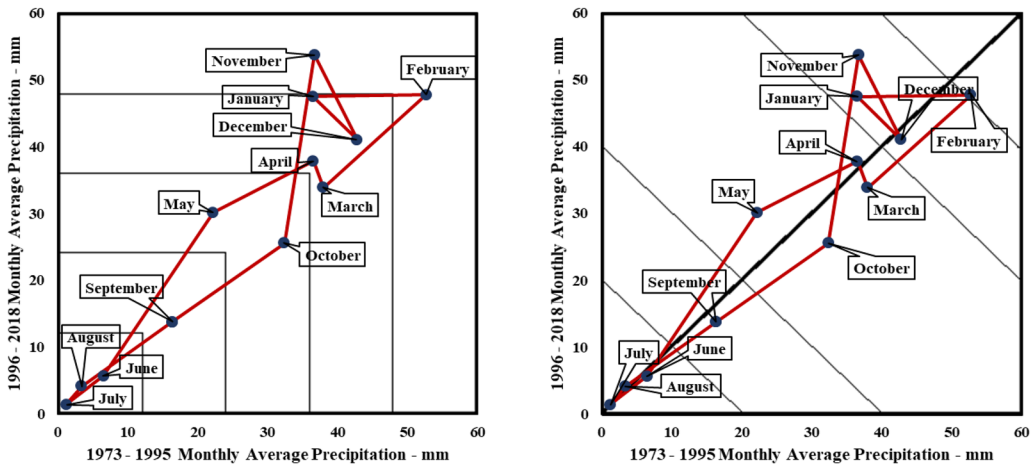

Bouzghaia Station

Benairia Station

Fig. 6 Arithmetic mean analysis results of ITPAM for each station
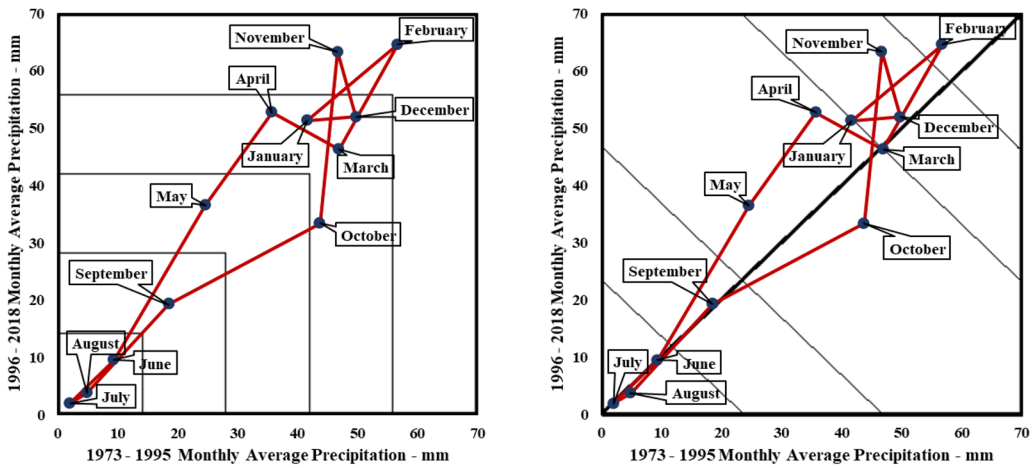
Fig. 6 (continued)

Table 3 General evaluation of arithmetic mean analysis results of ITPAM for each station

Stations	September	October	November	December	January	February	March	April	May	June	July	August
Larbat Ouled Fares												
Trend (Region-Range)	IT-LD	DT-MD	IT-HD	DT-HD	IT-HD	DT-HD	DT-HD	IT-MD	IT-MD	NT	NT	IT-VLD
Symbolic Trend Type	▲	▶	◀	◀	◀	◀	◀	▶	▶	—	—	▼
Risk Range	4th DRR	3rd DRR	1st DRR	1st DRR	1st DRR	1st DRR	2nd DRR	2nd DRR	3rd DRR	5th DRR	5th DRR	5th DRR
Bouzghaia												
Trend (Region-Range)	NT	DT-MD	IT-HD	IT-MD	IT-MD	DT-MD	DT-MD	IT-MD	NT	DT-VLD	NT	DT-VLD
Symbolic Trend Type	—	▶	◀	▶	▶	▶	▶	▶	—	▼	—	▼
Risk Range	5th DRR	3rd DRR	1st DRR	2nd DRR	3rd DRR	2nd DRR	3rd DRR	3rd DRR	4th DRR	5th DRR	5th DRR	5th DRR
Benairia												
Trend (Region-Range)	NT	DT-MD	IT-HD	IT-HD	IT-HD	DT-HD	DT-MD	IT-MD	IT-LD	DT-VLD	NT	NT
Symbolic Trend Type	—	▶	◀	◀	◀	◀	▶	▶	▲	▼	—	—
Risk Range	4th DRR	3rd DRR	1st DRR	2nd DRR	2nd DRR	2nd DRR	2nd DRR	3rd DRR	4th DRR	5th DRR	5th DRR	5th DRR
Medjaja												
Trend (Region-Range)	IT-LD	DT-MD	IT-HD	IT-HD	IT-HD	DT-HD	DT-MD	IT-MD	IT-MD	NT	NT	NT
Symbolic Trend Type	▲	▶	◀	◀	◀	◀	▶	▶	▶	—	—	—
Risk Range	4th DRR	3rd DRR	1st DRR	2nd DRR	2nd DRR	1st DRR	2nd DRR	3rd DRR	3rd DRR	5th DRR	5th DRR	5th DRR
Chettia												
Trend (Region-Range)	DT-LD	DT-MD	IT-HD	DT-HD	IT-HD	DT-VHD	DT-MD	IT-MD	IT-MD	NT	NT	IT-VLD
Symbolic Trend Type	◀	▶	◀	◀	◀	▲	▶	▶	▶	—	—	▼
Risk Range	4th DRR	3rd DRR	1st DRR	2nd DRR	2nd DRR	1st DRR	2nd DRR	2nd DRR	3rd DRR	5th DRR	5th DRR	5th DRR
Airport, Chlef												
Trend (Region-Range)	NT	DT-MD	IT-HD	IT-HD	IT-MD	IT-VHD	NT	IT-MD	IT-MD	NT	NT	NT
Symbolic Trend Type	—	▶	◀	◀	▶	▲	—	▶	▶	—	—	—
Risk Range	4th DRR	2nd DRR	1st DRR	2nd DRR	2nd DRR	1st DRR	2nd DRR	2nd DRR	3rd DRR	5th DRR	5th DRR	5th DRR

February and November fall inside the 1st degree of danger. For Airport, Chlef station, while April is in a region with a moderately growing trend, and October is in a region with a moderately dropping trend, the danger range is 2nd degree. In addition, February and November fall within the first degree of risk.
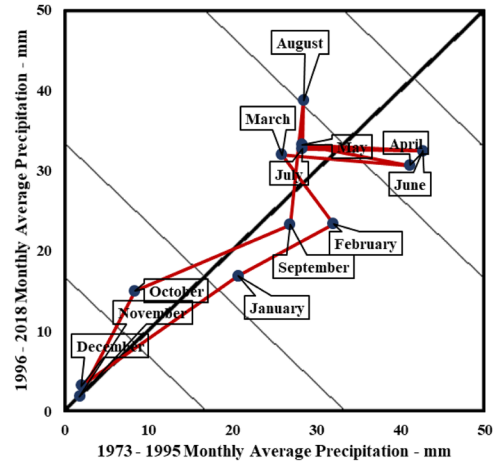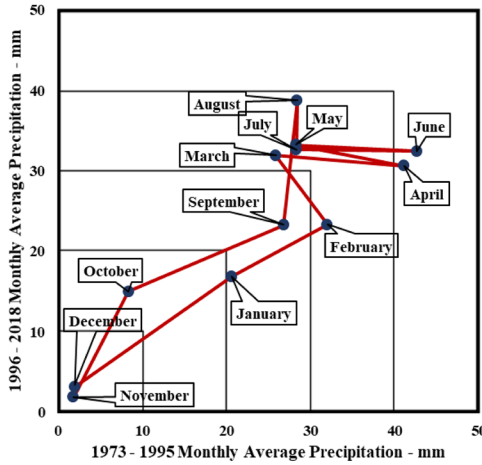
The ITPAM standard deviation analysis findings can be seen in Fig. 5. When Table 4's ITPAM standard deviation analysis results for each station are reviewed, the following information is acquired. Again, differences in the seasonal cycle of precipitation standard deviation and its trend between stations are evident as different polygon shapes. Increasing or decreasing trends are seen as the deviation from the 1:1 (45°) line. In general, February is a medium-degree decreasing trend region in contrast to May that is in a medium-degree increasing trend region. Meanwhile, no trend is seen in November for all stations.

Table 4 The general evaluation of standard deviation analysis results of each station

| Stations	September	October	November	December	January	February	March	April	May	June	July	August
Larbat Ouled Fares												
Trend (Region-Class)	DT-MD	IT-LD	NT	NT	DT-MD	DT-MD	IT-MD	DT-HD	IT-MD	DT-HD	IT-MD	IT-HD
Symbolic Trend Type	▶	▲	—	—	▶	▶	▶	◀	▶	◀	▶	▶
Risk Class	3rd DRC	4th DRC	5th DRC	5th DRC	3rd DRC	2nd DRC	2nd DRC	1st DRC	2nd DRC	1st DRC	2nd DRC	2nd DRC
Bouzghaia												
Trend (Region-Class)	IT-MD	NT	NT	IT-VLD	IT-LD	DT-MD	IT-MD	IT-HD	IT-MD	DT-HD	DT-MD	IT-MD
Symbolic Trend Type	▶	—	—	▼	▲	▶	▶	▶	▶	◀	▶	▶
Risk Class	3rd DRC	5th DRC	5th DRC	5th DRC	4th DRC	2nd DRC	1st DRC	2nd DRC	3rd DRC	1st DRC	3rd DRC	2nd DRC
Benairia												
Trend (Region-Class)	IT-MD	DT-VLD	NT	IT-VLD	DT-LD	DT-MD	IT-HD	DT-VHD	IT-MD	DT-HD	DT-MD	IT-MD
Symbolic Trend Type	▶	▼	—	▼	▲	▶	◀	▲	▶	◀	▶	▶
Risk Class	2nd DRC	5th DRC	5th DRC	5th DRC	4th DRC	3rd DRC	1st DRC	1st DRC	2nd DRC	1st DRC	2nd DRC	2nd DRC
Medjaja												
Trend (Region-Class)	IT-MD	IT-VLD	NT	IT-VLD	IT-LD	DT-MD	IT-MD	DT-HD	IT-MD	DT-VHD	IT-MD	NT
Symbolic Trend Type	▶	▼	—	▼	▲	▶	▶	◀	▶	▼	▶	—
Risk Class	3rd DRC	5th DRC	5th DRC	5th DRC	4th DRC	2nd DRC	2nd DRC	2nd DRC	2nd DRC	1st DRC	3rd DRC	2nd DRC
Chettia												
Trend (Region-Class)	IT-MD	IT-LD	NT	IT-VLD	DT-MD	DT-MD	IT-MD	DT-MD	IT-MD	DT-HD	IT-MD	IT-HD
Symbolic Trend Type	▶	▲	—	▼	▶	▶	▶	▶	▶	◀	▶	◀
Risk Class	2nd DRC	4th DRC	5th DRC	5th DRC	3rd DRC	2nd DRC	2nd DRC	3rd DRC	2nd DRC	1st DRC	3rd DRC	2nd DRC
Airport, Chlef												
Trend (Region-Class)	IT-MD	IT-LD	NT	NT	DT-MD	DT-MD	NT	IT-HD	IT-MD	DT-VHD	IT-MD	IT-HD
Symbolic Trend Type	▶	▲	—	—	▶	▶	—	◀	▶	▲	▶	◀
Risk Class	2nd DRC	4th DRC	5th DRC	5th DRC	3rd DRC	2nd DRC	2nd DRC	1st DRC	3rd DRC	1st DRC	2nd DRC	1st DRC
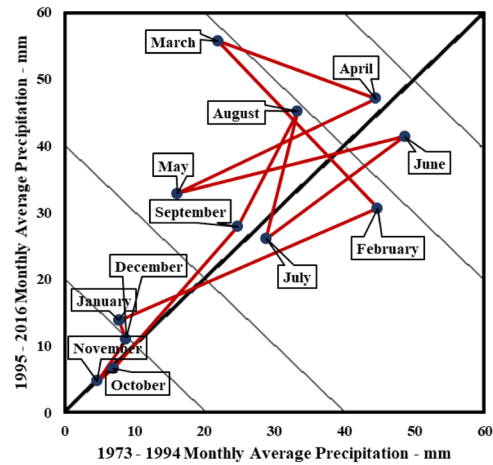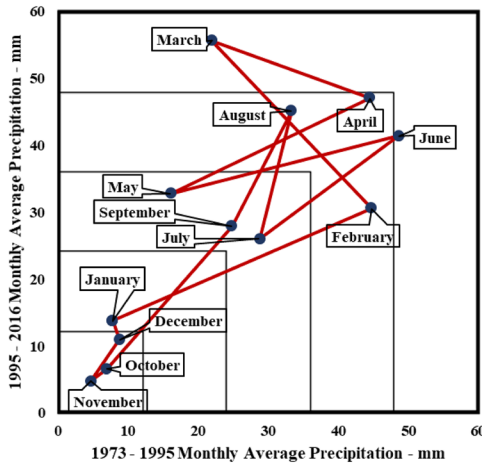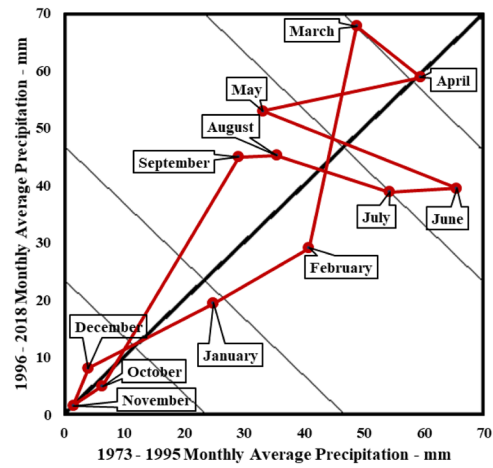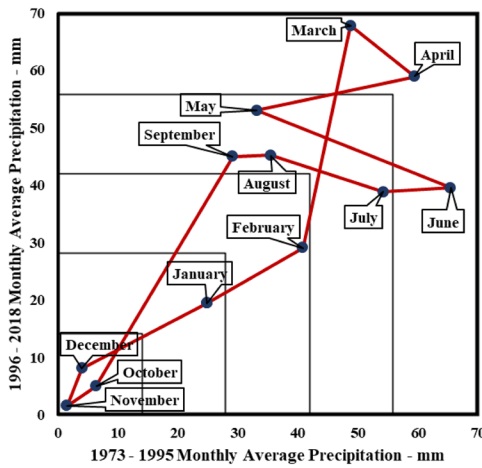
Fig. 7 Standard deviation analysis results of ITPAM for each station

Medjaja Station
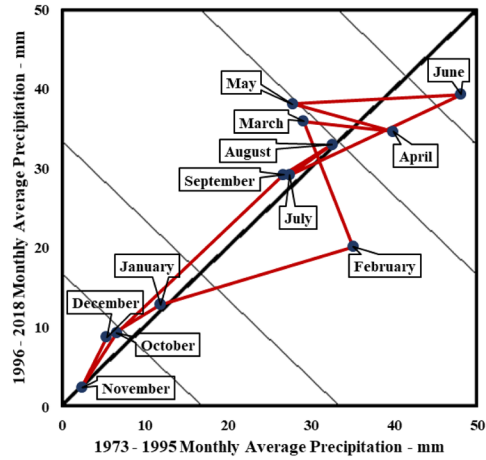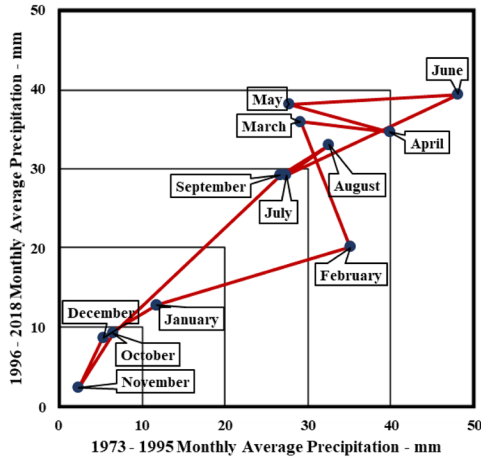
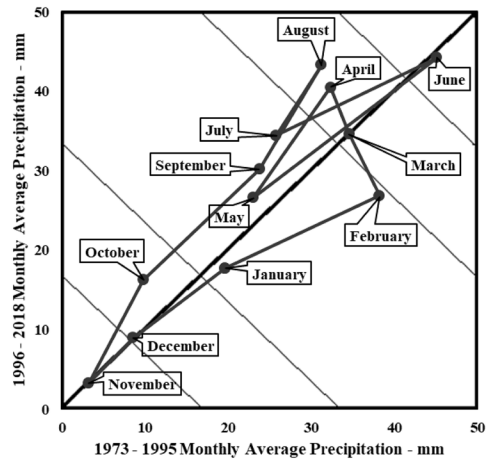
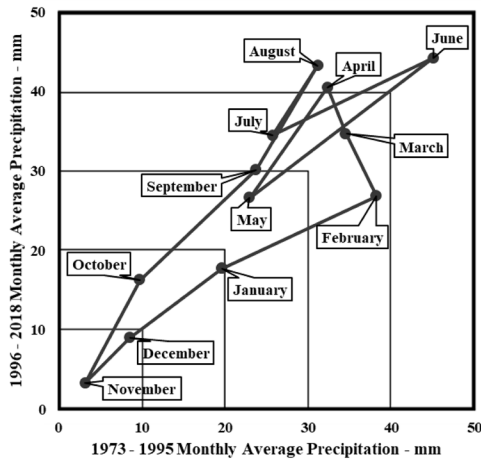## Chettia Station
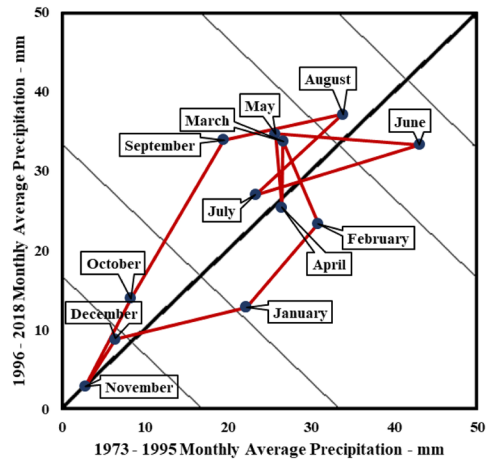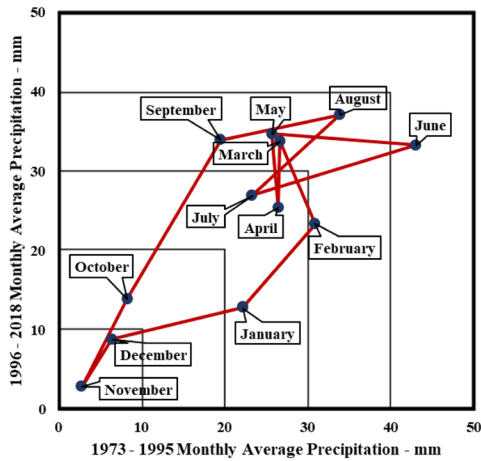
Airport, Chlef Station
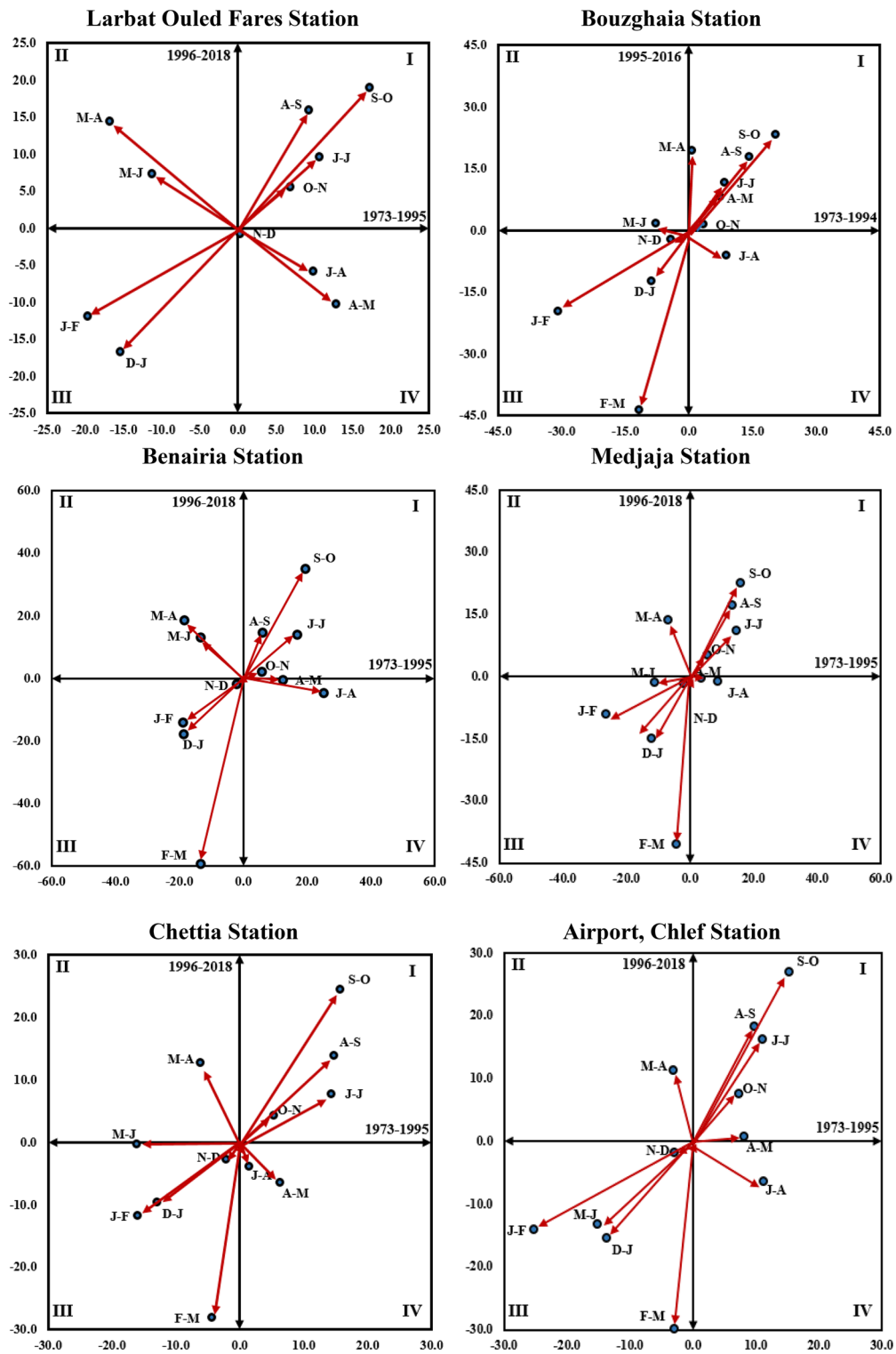

Fig. 7 (continued)

Fig. 8 Trend polygon star graphics of arithmetic mean analysis results for each station

June is in the 1st risk range as well as November and December are in the 5th risk range for all stations. For Larbat Ouled Fares station, while February, March, May, and July are in medium-degree increasing trend region, the risk range is 2nd degree. Moreover, April and June are in the 1st degree risk range. For Bouzghaia station, while February and August are in a medium-degree decreasing trend region, the risk range is 2nd degree. While March is in a medium-degree increasing trend region, the risk range is 1st degree. It is seen that there is a significant change between the two data sets for this month. Moreover, June is in the 1st degree risk range. For Benairia station, while May, August, and September are in a medium-degree decreasing trend region, the risk range is 2nd degree. Moreover, March, April, and June are in the 1st degree risk range. For Medjaja station, while February, March, and May are in a medium-degree decreasing trend region, the risk range is 2nd degree. Besides, June is in the 1st degree risk range. For Chettia station, while February, March, and May are in a medium-degree decreasing trend region, the risk range is 2nd degree. Additionally, June is in the 1st degree risk range. For Airport, Chlef station, while February and July are in medium-degree decreasing trend region, the risk range is 2nd degree. Furthermore, April, June, and August are in the 1st degree risk range.

The TPS method applied to monthly average precipitation data is also applied separately for both arithmetic mean and standard deviation. Arithmetic mean analysis results of TPS are given in Fig. 7.

When trend polygon star concept method arithmetic mean analysis results of six stations shown in Fig. 7 are examined, the following conclusions are reached. Arrows showing the transition between months J-J, A-S, S–O, and O-N of Larbat Ouled Fares station are in region I. Therefore, both data sets of these months show an increasing trend. Moreover, arrows showing the transition between J-F and D-J months are in region III. Therefore, both data sets of these months show a seasonal decrease trend. On the other hand, the longest arrow showing transition between the months is between S–O months, marking the transition between the dry and the wet season. Arrows showing the transition between months A-M, J-J, A-S, S–O, and O-N of Bouzghaia station are in region I, while arrows showing the transition between J-F, F-M, N-D, and D-J months are in region III.

While arrows in region I show an increasing trend for both data sets, arrows in region III show a decreasing trend. On the other hand, the longest arrow showing transition between the months is between F-M, marking the end of the wet season. It is seen that Benairia and Medjaja stations give similar results to the Bouzghaia station. On the other hand, the longest arrow is between F-M months. Arrows showing the transition between months J-J, A-S, S–O, and O-N of Chettia station are in region I. Therefore, both data sets of these months show an increasing trend. However, arrows showing the transition between J-F, F-M, M-J, N-D, and D-J months are in region III. Therefore, both data sets of these months show a decreasing trend. On the other hand, the longest arrow is between F-M and S–O months. It is seen that Airport, Chlef station gives similar results to the Chettia station. On the other hand, the longest arrow showing transition between the months in this station is between J-F, F-M, and S–O months. The March–April and May–June arrows are mostly in region II, highlighting that there may be a substantial change in precipitation distribution over the study period during the end of the rainy season in spring and early summer.

When TPS is applied to interannual standard deviation, for the six stations, the results are as shown in Fig. 8. Arrows showing the transition between months A-S, S–O, and O-N of Larbat Ouled Fares station are in region I. Therefore, both data sets of these months show an increasing trend. However, arrows showing the transition between J-F and D-J months are in region III. Therefore, both data sets of these months show a decreasing trend. On the other hand, the longest arrow showing transition between the months is between S–O and D-J months. Arrows showing the transition between months A-M, J-J, A-S, S–O, and O-N of Bouzghaia station are in region I. Arrows showing the transition between J-F, M-J, J-A, and N-D months are in region III. While arrows in the region I show an increasing trend for both data sets, arrows in region III show a decreasing trend. On the other hand, the longest arrow showing transition between the months is between J-F and F-M months. Moreover, the arrow showing transition between F-M months is in region IV. Therefore, the first dataset shows an increasing trend, while the second dataset shows a decreasing trend. It is seen that Benairia station gives similar results with Bouzghaia station. On the other hand, the longest arrow is between F-M and

Table 5 Statistical values of trend polygon star concepts method analysis results of the six precipitation observation stations

Larbat Ouled Fares		Sept-Oct	Oct-Nov	Nov-Dec	Dec-Jan	Jan-Feb	Feb-Mar	Mar-Apr	Apr-May	May-Jun	Jun-Jul	Jul-Aug	Aug-Sep
Arithmetic mean	Horizontal (mm)	**−19.7**	−4.1	−16.8	12.8	−11.2	10.7	9.9	9.3	17.3	6.9	0.3	−15.3
	Vertical (mm)	−11.9	**−26.3**	14.4	−10.3	7.3	9.6	−5.9	16.0	19.0	5.5	−0.7	−16.7
Standard deviation	Horizontal (mm)	−11.4	6.2	−15.3	12.9	−14.4	14.4	−0.1	1.6	18.5	6.6	−0.2	**−18.6**
	Vertical (mm)	−6.5	−8.6	1.3	−2.6	0.8	−0.2	−6.1	**15.5**	8.3	12.0	−0.2	−13.7
Bouzghaia		Sep-Oct	Oct-Nov	Nov-Dec	Dec-Jan	Jan-Feb	Feb-Mar	Mar-Apr	Apr-May	May-Jun	Jun-Jul	Jul-Aug	Aug-Sep
Arithmetic mean	Horizontal (mm)	**−30.8**	−11.8	0.7	7.4	−7.8	8.4	8.9	14.3	20.5	3.4	−4.2	−8.8
	Vertical (mm)	−19.7	**−43.6**	19.3	8.3	1.8	11.6	−6.1	18.0	23.3	1.6	−2.2	−12.2
Standard deviation	Horizontal (mm)	**−36.9**	22.8	−22.5	28.4	−32.5	19.8	−4.5	8.5	17.8	2.3	−4.1	1.0
	Vertical (mm)	−16.8	**−25.0**	8.6	14.2	−8.6	15.4	−19.1	17.2	21.3	2.0	−6.4	−2.8
Benairia		Sep-Oct	Oct-Nov	Nov-Dec	Dec-Jan	Jan-Feb	Feb-Mar	Mar-Apr	Apr-May	May-Jun	Jun-Jul	Jul-Aug	Aug-Sep
Arithmetic mean	Horizontal (mm)	−19.0	−13.4	−18.6	12.3	−13.4	6.0	**25.0**	16.8	19.5	5.7	−2.2	−18.7
	Vertical (mm)	−14.0	**−59.2**	18.7	−0.5	13.1	14.7	−4.6	14.1	35.1	2.2	−1.8	−17.8
Standard deviation	Horizontal (mm)	−15.9	−8.0	−10.7	26.3	**−32.3**	11.2	18.8	6.3	22.7	4.8	−2.5	−20.8
	Vertical (mm)	−9.6	**−38.7**	8.9	5.9	13.5	0.7	−6.4	0.3	40.0	2.6	−5.7	−11.3
Medjaja		Sep-Oct	Oct-Nov	Nov-Dec	Dec-Jan	Jan-Feb	Feb-Mar	Mar-Apr	Apr-May	May-Jun	Jun-Jul	Jul-Aug	Aug-Sep
Arithmetic mean	Horizontal (mm)	**−26.2**	−4.2	−6.8	3.5	−10.9	13.3	9.0	14.6	16.0	5.5	−1.8	−12.1
	Vertical (mm)	−9.2	**−40.4**	13.6	−0.4	−1.4	17.1	−1.1	11.1	22.5	5.1	−1.7	−15.1
Standard deviation	Horizontal (mm)	**−23.2**	6.0	−10.7	12.1	−20.3	20.7	−5.1	5.8	20.1	4.2	−3.0	−6.5
	Vertical (mm)	−7.3	−15.8	1.3	−3.5	−1.2	10.1	−3.8	3.8	**19.9**	6.2	−5.7	−4.1
Chettia		Sep-Oct	Oct-Nov	Nov-Dec	Dec-Jan	Jan-Feb	Feb-Mar	Mar-Apr	Apr-May	May-Jun	Jun-Jul	Jul-Aug	Aug-Sep
Arithmetic mean	Horizontal (mm)	−16.0	−4.3	−6.1	6.3	**−16.2**	14.7	1.4	14.3	15.7	5.3	−2.2	−13.0
	Vertical (mm)	−11.8	−28.1	12.7	−6.5	−0.3	13.9	−3.9	7.7	**24.4**	4.3	−2.7	−9.6
Standard deviation	Horizontal (mm)	−8.7	4.2	0.2	0.8	−17.3	**19.7**	−10.5	14.3	11.2	5.5	−3.6	−15.7
	Vertical (mm)	−10.5	−10.4	8.4	−9.3	1.4	6.3	−10.1	3.2	**20.0**	11.3	−6.2	−4.0
Airport, Chlef		Sep-Oct	Oct-Nov	Nov-Dec	Dec-Jan	Jan-Feb	Feb-Mar	Mar-Apr	Apr-May	May-Jun	Jun-Jul	Jul-Aug	Aug-Sep
Arithmetic mean	Horizontal (mm)	**−25.2**	−3.0	−3.1	8.1	−15.1	9.8	11.2	11.1	15.3	7.3	−2.9	−13.6
	Vertical (mm)	−14.1	−29.9	11.3	0.7	−13.3	18.2	−6.4	16.2	**27.0**	7.6	−1.8	−15.5
Standard deviation	Horizontal (mm)	−18.6	3.7	2.2	9.3	−22.1	**19.3**	−5.4	7.4	14.0	6.6	−5.4	−11.1
	Vertical (mm)	−9.1	−7.8	−5.8	13.9	**−17.6**	9.8	−8.8	13.1	13.9	12.7	−5.4	−8.7

Bold entries show the maximum value of C

S–O months. Arrows showing the transition between months J-J, A-S, S–O, and O-N of Medjaja station are in region I. Therefore, both data sets of these months show an increasing trend. However, arrows showing the transition between J-F, M-J, J-A, N-D, and D-J months are in region III. Therefore, both data sets of these months show a decreasing trend. On the other hand, the longest arrow showing transition between the months is between S–O months. It is seen that Chettia station gives similar results with Medjaja station. Only the arrow showing transition between F-M months is in region IV. On the other hand, the longest arrow is between J-F and S–O months. Arrows showing the transition between months A-M, J-J, A-S, S–O, and O-N in Airport, Chlef station are in region I. There are no arrows in region II. Arrows showing the transition between months J-F, M-J, J-A, N-D, and D-J are in region III. Arrows in the region I show an increasing trend, while arrows in region III show a decreasing trend. The longest arrow is between M-J. As with the mean precipitation, large changes in standard deviation between halves of the study period are seen especially for the end of the rainy season in the spring, suggesting possible hydrologic intensification and elevated interannual variability particularly in this season over recent decades.
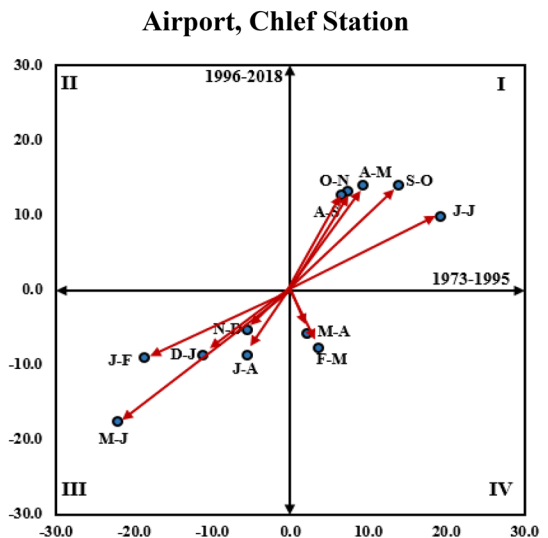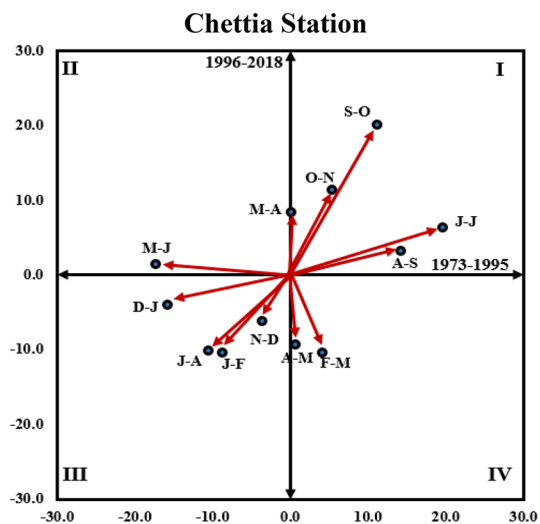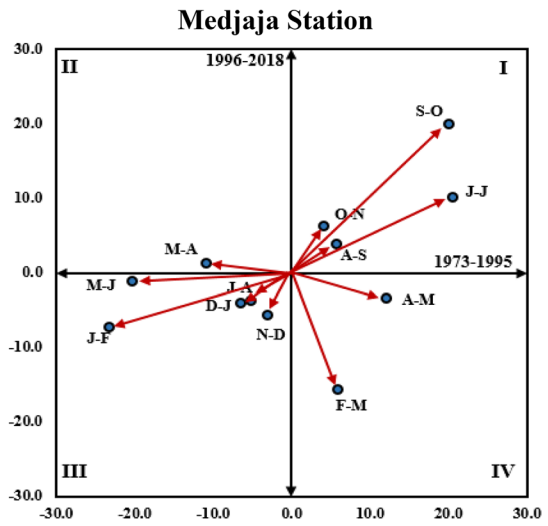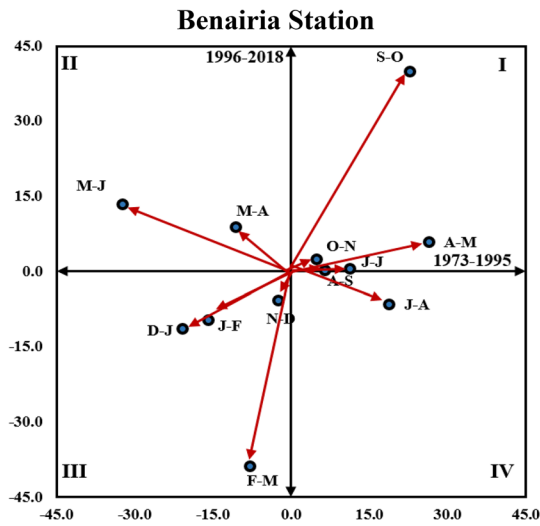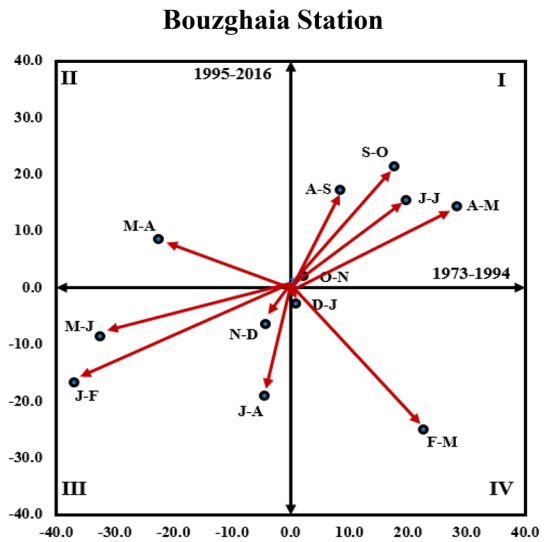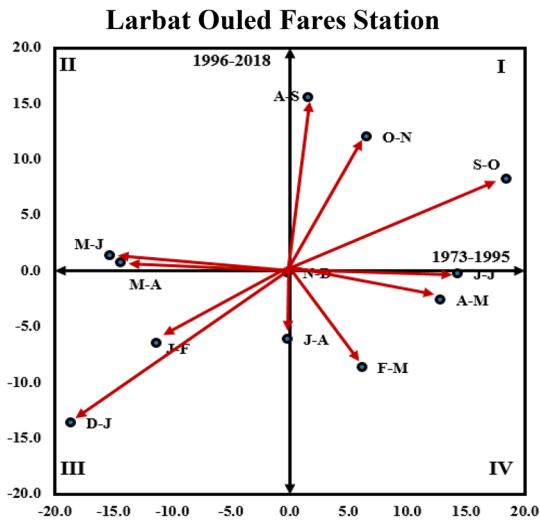
A tabular summary of TPS for six stations is provided in Table 5. The bold values show the maximum transition between two months. For example, when results for Benairia station are examined, it shows that maximum horizontal is between March and April for arithmetic average and between January and February for standard deviation, reflecting the end of the rainy season. The maximum vertical shows that it is between October and November for both the arithmetic mean and the standard deviation reflecting the beginning of the rainy season Fig. 9.

Discussion

The results of IPTAM methods are very helpful in water resource management mainly in regard to agricultural sector, as they supplement standard hydroclimatic analyses in highlighting the seasonality of precipitation trends. In fact, past studies on rainfall trend performed in Algeria evidenced a significant decrease in the annual amount since the 1970s. For example, Khedimallah et al. (2020) applied the Mann–Kendal

and Pettitt tests and detected significant downward trends for rainfall in the Cheliff and in the Medjerda basins in the period 1968–2013, while Taibi et al. (2017) using the Mann–Kendall test and the Theil Sen estimator showed that a severe drought affected the western, western highland, and Cheliff regions since the mid-1970s. Conversely, in this study, the application of the IPTAM method evidenced increasing trends of precipitation in autumn and winter seasons, like in Larbat, Bouzghaia, Benairia, Medjaja, and Chettia stations, which can promote increased water storage in soil useful in vegetation season. The spring precipitation has generally lower mean precipitation and interannual standard deviation but showed some consistent changes in seasonality between halves of the study period that should be examined more closely for statistical significance and physical driving mechanisms. These results are quite similar to the ones presented by Achite and Caloiero (2021) that using two non-parametric tests evidenced a positive trend in autumn in the Wadi Sly basin, or by Abu Hammad et al. (2022), which evidenced an increase in winter precipitation in the Eastern Mediterranean. This monthly behavior can be explained by local enforcement in the intensity of cyclogenesis events in the Mediterranean region. Extreme decreasing trend in summer precipitation (June, July, and August) can accelerate drought and water scarcity not only for agriculture but also for people (Tolba & Najib, 2009). Changes of temperature and precipitation in this region can be affected by the South Asian summer monsoon (SASM) through the monsoon–desert teleconnection (Kim et al., 2019).

Serinaldi et al. (2020) performed a series of numerical experiments to show the limitations of ITA and related methods. In particular, they evidenced that the ITA method has high type 1 error rates in critical trend value. In order to overcome such a problem, recently several improvements on the ITA methods have been proposed. For example, Alashan (2020) suggested the ITA_R to determine critical trend values as to whether they are significant according to a certain statistical significance level. In order to enhance the visual aspect of the ITA method, Alashan (2018) proposed the innovative trend analysis change boxes (ITA-CB) approach. The double-ITA (D-ITA) and triple-ITA (T-ITA) procedures were suggested for the trend stability assessment by comparing partial trend components during different

Larbat Ouled Fares Station

Bouzghaia Station

Benairia Station

Medjaja Station

Chettia Station

Airport, Chlef Station

◄**Fig. 9** Trend polygon star concepts method graphics of standard deviation analysis results for each station

sub-periods of a given record series (Güçlü, 2018; Zerouali et al., 2022). Finally, with the aim to identify partial trends and to determine the stability and/or periodicity of these trends in a given time series, Güçlü et al. (2020) developed the innovative triangular trend analysis (ITTA). In this context, we caution that the ITRA, ITPAM, and TPS methods should be used only as a qualitative tool to support other methods when detecting the trend of hydrometeorological data. Some aspects of the ITRA, ITPAM, and TPS methods could be modified to improve their usefulness for visualizing precipitation trends in semiarid Mediterranean regions. For example, a measure of statistical significance of trends could be added to the plots, perhaps based on tests that take serial correlation into account. The number and levels of "risk zones" could be also customized based on local hydrologic knowledge as opposed to being set in an automated way from the range in the data.

Conclusions

In this study, precipitation data of the Wadi Ouahrane basin of Algeria were analyzed using the ITRA, ITPAM, and TPS methods. The following main results were obtained:

1. ITRA graphs show the direction of the precipitation trend (increasing–decreasing) and the trend risk class.
2. Disparities in the polygons generated by the arithmetic mean and standard deviation ITPAM graphs demonstrate variations in precipitation seasonally and in the seasonal precipitation trends (increasing or decreasing) between sites.
3. The TPS maps depict monthly variations in precipitation and highlight the autumn and spring transitions between the dry and wet seasons.
4. In the analysis results of the ITRA method, less trend is seen in low and medium precipitation regimes, and it has been observed that there are imbalances in high precipitation regimes.
5. The application of the IPTAM method evidenced an increasing trend of precipitation in autumn and winter.

6. The spring precipitation has generally lower mean precipitation and interannual standard deviation but showed some consistent changes in seasonality between halves of the study period.

In order to better appreciate the results of this study, important final remarks must be made concerning the strength and the weaknesses of this research. In fact, although the application of the ITRA, ITPAM, and TPS allows us to overcome one of the main limitations of classical trend analysis, i.e., the lack of information about the transition of hydroclimatic variables between months, we suggest to use these methods only as a qualitative tool to support other methods when detecting the trend of hydrometeorological data due to the lack of a measure of statistical significance of trends. Anyway, the results of this study are particularly relevant because the evaluated changes in rainfall could impact on agriculture production, affecting the soil, hydrology, and plant health of agricultural systems, and thus, it is important to try to extend in the future these analyses to other northern Algerian basins.

Declarations

Competing interests The authors declare no competing interests.

References

Abu Hammad, A. H. Y., Salameh, A. A. M., & Fallah, R. Q. (2022). Precipitation variability and probabilities of extreme events in the eastern Mediterranean region (Latakia governorate-Syria as a case study). *Atmosphere, 13*, 131.

Achite, M., Ceribasi, G., Ceyhunlu, A. I., Wałęga, A., & Caloiero, T. (2021a). The innovative polygon trend analysis (IPTA) as a simple qualitative method to detect changes in environment—Example detecting trends of the total monthly precipitation in semiarid area. *Sustainability, 13*(22), 12674.

Achite, M., Wałęga, A., Toubal, A. K., Mansour, H., & Krakauer, N. (2021b). Spatiotemporal characteristics and trends of meteorological droughts in the Wadi Mina basin. *Northwest Algeria. Water, 13*(21), 3103.

Achite, M., & Caloiero, T. (2021). Analysis of temporal and spatial rainfall variability over the Wadi Sly basin. *Algeria. Arabian Journal of Geosciences, 14*, 1867.

Alashan, S. (2018). An improved version of innovative trend analyses. *Arabian Journal of Geosciences, 11*, 50.

Alashan, S. (2020). Testing and improving type 1 error performance of Şen's innovative trend analysis method. *Theoretical and Applied Climatology, 142*, 1015–1025.

Ali, R. O., & Abubaker, S. R. (2019). Trend analysis using Mann-Kendall, Sen's slope estimator test and innovative trend analysis method in Yangtze River basin, China. *International Journal of Engineering & Technology, 8*(2), 110–119.

Almazroui, M., & Şen, Z. (2020). Trend analyses methodologies in hydro-meteorological records. *Earth Systems and Environment, 4*(4), 713–738.

Asadieh, B., & Krakauer, N. Y. (2015). Global trends in extreme precipitation: Climate models versus observations. *Hydrology and Earth System Sciences, 19*(2), 877–891.

Blain, G. C. (2013). The Mann-Kendall test: The need to consider the interaction between serial correlation and trend. *Acta Scientiarum. Agronomy, 35*(4), 393–402.

Ceribasi, G., & Ceyhunlu, A. I. (2021). Analysis of total monthly precipitation of Susurluk Basin in Turkey using innovative polygon trend analysis method. *Journal of Water and Climate Change, 12*(5), 1532–1543.

Ceribasi, G., Ceyhunlu, A. I., & Ahmed, N. (2021a). Innovative trend pivot analysis method (ITPAM): A case study for precipitation data of Susurluk Basin in Turkey. *Acta Geophysica, 69*(4), 1465–1480.

Ceribasi, G., Ceyhunlu, A. I., & Ahmed, N. (2021b). Analysis of temperature data by using innovative polygon trend analysis and trend polygon star concept methods: A case study for Susurluk Basin. *Turkey. Acta Geophysica, 69*(5), 1949–1961.

Collins, M., Knutti, R,, Arblaster, J., Dufresne, J. L., Fichefet, T., Friedlingstein, P., & Booth, B. B. (2013). Long-term climate change: Projections, commitments and irreversibility. In: Proceedings of Climate Change 2013-The Physical Science Basis: Contribution of Working Group I to the Fifth Assessment Report of the Intergovernmental Panel on Climate Change. *Cambridge University Press,* 1029–1136.

Croitoru, A. E., & Toma, F. M. (2010). Trends in precipitation and snow cover in central part of Romanian plain. *Geographia Technica, 9*(1), 1–10.

Door, J. P. (2011). *Rapport d'information déposé en application de l'article 145 du règlement par la commission des affaires sociales en conclusion des travaux de la mission sur le Médiator et la pharmacovigilance*. Assemblée nationale.

Güçlü, Y. S. (2018). Multiple Şen-innovative trend analyses and partial Mann-Kendall test. *Journal of Hydrology, 566*, 685–704.

Güçlü, Y. S., Şişman, E., & Dabanlı, İ. (2020). Innovative triangular trend analysis. *Arabian Journal of Geosciences, 13*(1), 1–8.

Harka, A. E., Jilo, N. B., & Behulu, F. (2021). Spatial-temporal rainfall trend and variability assessment in the Upper Wabe Shebelle River Basin, Ethiopia: Application of innovative trend analysis method. *Journal of Hydrology: Regional Studies, 37*, 100915.

Hu, Y., & Wang, S. (2021). Associations between winter atmospheric teleconnections in drought and haze pollution over Southwest China. *Science of the Total Environment, 766*, 142599.

Khedimallah, A., Meddi, M., & Mahé, G. (2020). Characterization of the interannual variability of precipitation and runoff in the Cheliff and Medjerda basins (Algeria). *Journal of Earth System Science, 129*, 1–25.

Kim, G. U., Seo, K. H., & Chen, D. (2019). Climate change over the Mediterranean and current destruction of marine ecosystem. *Scientific Reports, 9*(1), 1–9.

Kingston, D. G., Stagge, J. H., Tallaksen, L. M., & Hannah, D. M. (2015). European-scale drought: Understanding connections between atmospheric circulation and meteorological drought indices. *Journal of Climate, 28*(2), 505–516.

Kisi, O., & Ay, M. (2014). Comparison of Mann-Kendall and innovative trend method for water quality parameters of the Kizilirmak River, Turkey. *Journal of Hydrology, 513*, 362–375.

Littmann, T. (2000). An empirical classification of weather types in the Mediterranean Basin and their interrelation with rainfall. *Theoretical and Applied Climatology, 66*(3), 161–171.

Meddi, M. M., Assani, A. A., & Meddi, H. (2010). Temporal variability of annual rainfall in the Macta and Tafna catchments. *Northwestern Algeria. Water Resources Management, 24*(14), 3817–3833.

Młyński, D., Cebulska, M., & Wałęga, A. (2018). Trends, variability, and seasonality of maximum annual daily precipitation in the upper Vistula basin. *Poland. Atmosphere, 9*(8), 313.

Nishant, N., & Sherwood, S. C. (2021). How strongly are mean and extreme precipitation coupled? *Geophysical Research Letters, 48*(10), e2020GL092075.

Onyutha, C. (2016). Identification of sub-trends from hydro-meteorological series. *Stochastic Environmental Research and Risk Assessment, 30*(1), 189–205.

Pendergrass, A. G., & Hartmann, D. L. (2014). Changes in the distribution of rain frequency and intensity in response to global warming. *Journal of Climate, 27*(22), 8372–8383.

Praveen, B., Talukdar, S., Shahfahad, et al. (2020). Analyzing trend and forecasting of rainfall changes in India using non-parametrical and machine learning approaches. *Scientific Report, 10*, 10342.

Şen, Z. (2012). Innovative trend analysis methodology. *Journal of Hydrologic Engineering, 17*(9), 1042–1046.

Şen, Z. (2013). Trend identification simulation and application. https://doi.org/10.1061/(ASCE)HE.1943-5584.0000811. Received: March 14, 2012. Accepted: February 28, 2013. Published online: March 04, 2013.

Şen, Z. (2021). Conceptual monthly trend polygon methodology and climate change assessments. *Hydrological Sciences Journal, 66*(3), 503–512.

Serinaldi, F., Chebana, F., & Kilsby, C. G. (2020). Dissecting innovative trend analysis. *Stochastic Environmental Research and Risk Assessment, 34*(5), 733–754.

Serinaldi, F., Kilsby, C. G., & Lombardo, F. (2018). Untenable nonstationarity: An assessment of the fitness for purpose of trend tests in hydrology. *Advances in Water Resources, 111*, 132–155.

Taibi, S., Meddi, M., Mahé, G., & Assani, A. (2017). Relationships between atmospheric circulation indices and rainfall in Northern Algeria and comparison of observed and

RCM-generated rainfall. *Theoretical and Applied Climatology, 127*, 241–257.

Tolba, M. K. S., & Najib, W. (2009). Arab environment: Climate change: Impact of climate change on Arab countries. Arab Forum for Environment and Development (AFED), Beirut, Lebanon.

Toreti, A., Naveau, P., Zampieri, M., Schindler, A., Scoccimarro, E., Xoplaki, E., & Luterbacher, J. (2013). Projections of global changes in precipitation extremes from coupled model intercomparison project phase 5 models. *Geophysical Research Letters, 40*(18), 4887–4892.

Tramblay, Y., El Adlouni, S., & Servat, E. (2013). Trends and variability in extreme precipitation indices over Maghreb countries. *Natural Hazards and Earth System Sciences, 13*(12), 3235–3248.

Turki, I., Laignel, B., Massei, N., Nouaceur, Z., Benhamiche, N., & Madani, K. (2016). Hydrological variability of the Soummam watershed (Northeastern Algeria) and the possible links to climate fluctuations. *Arabian Journal of Geosciences, 9*(6), 1–12.

Wang, F., Shao, W., Yu, H., Kan, G., He, X., Zhang, D., & Wang, G. (2020). Re-evaluation of the power of the Mann-Kendall test for detecting monotonic trends in hydrometeorological time series. *Frontiers in Earth Science, 14*.

Yue, S., & Wang, C. (2004). The Mann-Kendall test modified by effective sample size to detect trend in serially correlated hydrological series. *Water Resources Management, 18*(3), 201–218.

Zeroual, A., Assani, A. A., & Meddi, M. (2017). Combined analysis of temperature and rainfall variability as they relate to climate indices in Northern Algeria over the 1972–2013 period. *Hydrology Research, 48*(2), 584–595.

Zerouali, B., Mesbah, M., Chettih, M., & Djemai, M. (2018). Contribution of cross time-frequency analysis in assessment of possible relationships between large-scale climatic fluctuations and rainfall of northern central Algeria. *Arabian Journal of Geosciences, 11*, 1–23.

Zerouali, B., Elbeltagi, A., Al-Ansari, N., Abda, Z., Chettih, M., Santos, C. A. G., et al. (2022). Improving the visualization of rainfall trends using various innovative trend methodologies with time-frequency-based methods. *Applied Water Science, 12*(9), 1–19.

Zhang, X., Wan, H., Zwiers, F. W., Hegerl, G. C., & Min, S. K. (2013). Attributing intensification of precipitation extremes to human influence. *Geophysical Research Letters, 40*(19), 5252–5257.

Zhang, Y., & Wu, R. (2021). Asian meteorological droughts on three time scales and different roles of sea surface temperature and soil moisture. *International Journal of Climatology, 41*(13), 6047–6064.

Zhao, Y., Xu, X., Huang, W., Wang, Y., Xu, Y., Chen, H., & Kang, Z. (2019). Trends in observed mean and extreme precipitation within the Yellow River Basin. *China. Theoretical and Applied Climatology, 136*(3), 1387–1396.